

Mitigation of Stimulated Raman Scattering in Hohlraum Plasmas

J. L. Kline,¹ D.S. Montgomery,¹ H. A. Rose,¹ S. R. Goldman,¹ D. H. Froula,²
J. S. Ross,² R. M. Stevenson³ and P. M. Lushnikov⁴

- 1) Los Alamos National Laboratory, Los Alamos, NM 87545, USA
- 2) Lawrence Livermore National Laboratory, Livermore, California 94551, USA
- 3) Atomic Weapons Establishment, Aldermaston, Reading RG7 4PR, UK
- 4) Department of Mathematics, University of New Mexico, Albuquerque, NM, USA

Email: jkline@lanl.gov

Abstract. One aspect of recent research to control Stimulated Raman Scattering (SRS) in hohlraum plasmas is the investigation of risk mitigation strategies for indirect drive inertial confinement fusion. Experimental tests of these strategies, based on prior theoretical and experimental knowledge of SRS, are performed in hohlraum experiments. In the last year, two strategies have been investigated. The first is the use of high Z dopants to reduce SRS backscatter. Forward stimulated Brillouin scattering (FSBS) could lead to beam spray reducing SRS. Since FSBS depends on the electron temperature and thermal effects depend strongly on Z^2 , a small amount of a high Z dopant, 1-2%, can have a large effect. Experiments have been conducted at the Omega laser to test this theory by varying the amount of Xe dopant in neo-pentane gas filled hohlraums. The experimental measurements do show a decrease in SRS backscatter as Xe dopant is added. However, there are still uncertainties regarding the responsible mechanism since increases inverse-Bremsstrahlung absorption of the SRS light may play a role. The second strategy investigated is using high $k\lambda_D$ plasmas to reduce SRS backscatter. Experiments conducted at the Omega laser facility in hohlraum plasmas determined the critical onset intensity for a range of $k\lambda_D$. A scaling of the critical onset intensity as a function of $k\lambda_D$ has been determined.

1. Introduction

Gas filled hohlraums are often used for high energy density laser experiments including inertial confinement fusion. While the gas fill is needed to hold the ablated wall material for filling the hohlraum, it introduces a new set of problems. Coupling of the laser to the plasma causes laser plasma instabilities that can decrease the energy coupling to the target, affect the pointing of the beams, or generate hot electrons which preheat the target. One instability detrimental to gas filled hohlraum experiments is stimulated Raman Scattering (SRS) which occurs when intense laser light resonantly decays into an electron plasma wave and a backscattered light wave. Two strategies for mitigating SRS have recently been investigated at the University of Rochester Omega laser facility in gas filled hohlraums. The first strategy uses a small amount of a high-Z dopant in the low-Z gas fill, which had previously been observed to reduce SRS in experiments at the Helen laser.[1] The second strategy uses

lower density gas fills to increase Landau damping via the dimensionless parameter $k\lambda_D$. For the high Z dopants, there are two hypotheses for explaining the reduction of SRS reflectivity. A trivial explanation is that inverse-Bremsstrahlung absorption increases with the addition of high-Z dopant, thus showing a reduction in the measured SRS backscattered energy with the addition of high-Z dopant. A second explanation is that the high Z dopant induces beam spray via thermal Filamentation,[1, 2] or Forward Stimulation Brillouin Scattering[3-6], and affects the growth of SRS due to shorter correlation lengths within the laser beam. To examine the effects of high $k\lambda_D$ regimes on SRS, the critical onset intensity for SRS is measured.[7] A critical onset occurs theoretically for a random phase plate smoothed laser beam with a distribution of intensities with a well-defined spatial correlation length (speckle length). As the average laser intensity increases, the calculated SRS gain diverges leading to a saturated reflectivity. This is experimentally determined by measuring a sharp increase from no reflectivity to large reflectivity for a small increase in laser intensity. As $k\lambda_D$ increases, Landau damping of the electron plasma wave increases, thus increasing the SRS critical onset intensity. In this manuscript, we present experimental results for both the high Z dopant and large $k\lambda_D$ mitigation strategies for SRS in NIF relevant hohlraum plasmas.

2. Experimental Setup

Both sets of mitigation experiments were conducted at the Omega laser facility using gold hohlraums of the same dimensions. The gold hohlraums are cylindrical with the dimensions of 1.6 mm in diameter, 2.0 mm in length, and 25 μm wall thickness. A laser entrance hole (LEH) exists at both ends of the cylinder with an opening that is 50% of the cylinder diameter, i.e. 0.8 mm in diameter. 0.25 μm thick polyimide windows cover the LEH and seal the gas in the hohlraum. The hohlraums are filled with ~ 1 atmosphere of various $\text{C}_n\text{H}_{2n+2}$ mixtures. For the high Z dopant experiments, a small amount of Xe was also added, up to 9% atomic fraction. 32 laser beams of 351 nm light are used to create and heat the plasma. The heater beams used a 1 ns square pulse (SG1018). The 32 beams are pointed towards the wall of the hohlraum forming three cones with respect to the hohlraum axis. The maximum energy in each beam is 380 J, which is the maximum allowable when smoothing by spectral dispersion (SSD) is on. The total incident energy in the hohlraum is ~ 12 kJ. For the heater beams, random phase plates are not used, but the distributed polarization rotators (DPRs) are in the beam lines, which produces minimal effects on the heater beam intensity. All of the heater beams have the same timing except two, one on either side of the hohlraum. These two beams are initiated 0.5 ns ahead of the other heater beams and defocused to burn through the windows.

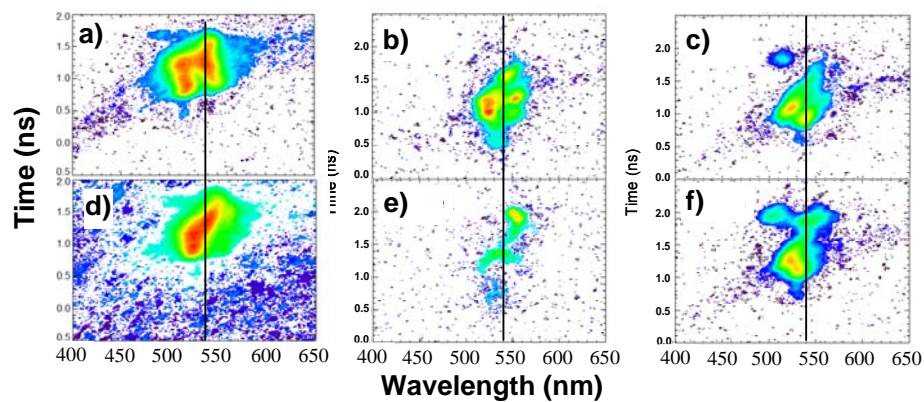


Figure 1: a) SRS spectrum for an $I_0 \sim 1.8 \times 10^{15}$ W/cm², SSD on, and %0 Xe dopant. b) SRS spectrum for an $I_0 \sim 1.0 \times 10^{15}$ W/cm², SSD on, and %0 Xe dopant. c) SRS spectrum for an $I_0 \sim 1.0 \times 10^{15}$ W/cm², SSD off, and %0 Xe dopant. d) SRS spectrum for an $I_0 \sim 1.8 \times 10^{15}$ W/cm², SSD on, and %9 Xe dopant. e) SRS spectrum for an $I_0 \sim 1.0 \times 10^{15}$ W/cm², SSD on, and %9 Xe dopant. f) SRS spectrum for an $I_0 \sim 1.0 \times 10^{15}$ W/cm², SSD off, and %9 Xe dopant.

The hohlraum is aligned along beamline 30, the LPI interaction beam. Beam 30 uses a phase plate that produces a 150 μm diameter spot size with an $f/6.7$ beam cone. For the target shots, the 2D SSD is both turned on and off, and different laser intensities are used. Beam 30 backscattered energy and spectra are measured using the full aperture backscattering diagnostic and the near backscatter imager.

3. SRS backscatter dependence on Xe dopant

Investigation of the effects of high Z dopant on SRS at the Omega laser has demonstrated a reduction in SRS with increasing high Z dopant measured in the SRS backscattered spectra. For these experiments, different amounts of Xe dopant by molecular fraction were added to the neo-pentane (C_5H_{12}) gas fill hohlraum target. Measurements were made for three different interaction beam conditions, high intensity with SSD at $I_0 \sim 1.8 \times 10^{15} \text{ W/cm}^2$, low intensity with SSD at $1.0 \times 10^{15} \text{ W/cm}^2$, and low intensity without SSD $1.0 \times 10^{15} \text{ W/cm}^2$. The backscattered spectra for each of the three aforementioned cases are shown in Figure 1 for two different amounts of Xe dopant, 0% and 9%. Figure 1a illustrates a challenge in analyzing the effects of the high Z dopants. The SRS backscattered light spectrum is bimodal with scattered light at $\sim 550 \text{ nm}$ and at $\sim 520 \text{ nm}$. The backscattered laser light near 550 nm is consistent with electron densities calculated based on the gas fill pressure measured at the time of the shot. The backscattered light near 520 nm is at a low density possibly from either the window or the plasma expanding from the hohlraum. The large amount of backscattered energy from this lower density region precludes the wavelength and time integrated backscattered energy measurement from directly being used. To determine the effects of high Z dopant due to the plasma in the interior of the hohlraum, the backscattered light spectra were converted to physical units of $\text{J}/(\text{s}\cdot\text{nm})$ and integrated over a wavelength range of 540-565 nm to produce a time dependent backscattered power measurement from plasma at the gas-fill density. While the bimodal effect is still present for the lower intensity case with SSD (Figure 1 b), high Z dopants appear to affect SRS over the entire wavelength range (Figure 1e). However, the same analysis technique is applied. When SSD was turned off most of the backscattered laser light occurred at wavelengths less than 540 nm suggesting that this backscattered light comes from the plasma blow off region. Little effect of high Z dopants was observed for this case, suggesting that SSD may be required for proper laser propagation into the hohlraum at this plasma density. It should be noted that the lower intensity was chosen to be near the measured critical onset intensity for SRS of $0.7 \times 10^{15} \text{ W/cm}^2$ in C_5H_{12} filled hohlraums.

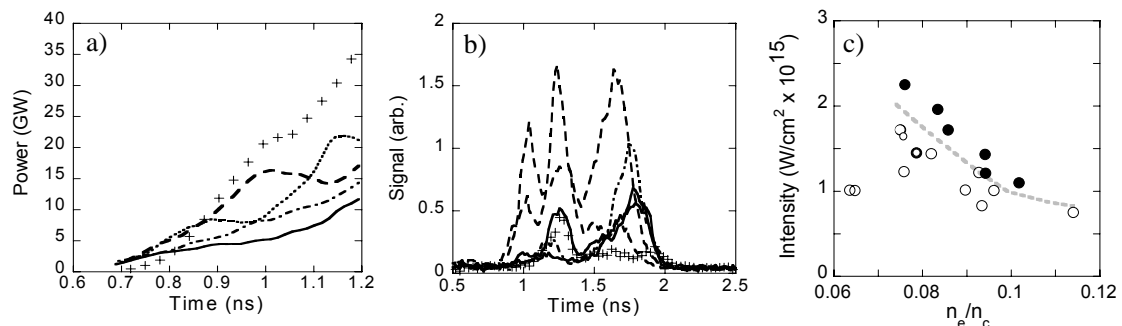


Figure 2: a) time dependent reflectivity for (---) 0%, (+++) 1.8%, (····) 3.6%, (- · -) 5.6%, and (—) 9% Xe dopant for an $I_0 \sim 1.8 \times 10^{15} \text{ W/cm}^2$ with SSD, on spectrally integrated from 540 – 580 nm, wavelengths that correspond to plateau density in hohlraum. b) time dependent reflectivity for 0%, 1%, 3%, 6%, and 9% Xe dopant for an $I_0 \sim 1.0 \times 10^{15} \text{ W/cm}^2$ with SSD on spectrally integrated from 540 – 565 nm, wavelengths that correspond to plateau in hohlraum. c) laser beam intensity versus n_e/n_c showing regions of (●) high (> 10%) and (○) low SRS (< 1%) due to the critical onset intensity.

Figures 2a and b show the time dependent backscattered light energy integrated over the wavelength band centered at 550 nm for different fractions of Xe dopant. For the high intensity case with SSD, the

time dependent backscattered energy is reduced as high Z dopant is added. The same effect is shown even more dramatically for the lower intensity case in Figure 2b. In both cases, there is a clear reduction in SRS backscatter from the interior of the hohlraum as Xe is added. Unfortunately, the dynamic nature of the hohlraum plasma makes de-convolving the effects of the Xe dopant challenging. For example, the interaction beam is delayed relative to the heater beams, so the large reflectivities seen in the backscattered light may result from a cooling plasma or the gold walls filling the hohlraum. To quantify the effects of the Xe dopant in these experiments, radiation hydrodynamic simulations are underway to gain more insight into the plasma dynamics. With a better understanding of the hydrodynamics, it may be possible to understand how the Xe dopant affects SRS and determine if either the reduced SRS backscatter light energy is simply due to inverse-Bremsstrahlung absorption or to what extent thermally-enhanced FSBS is responsible for the reduction in SRS.

4. $k\lambda_D$ scaling of the critical onset intensity for SRS

For laser beams focused through a random phase plate to smooth the beam, the laser far field pattern is comprised of many speckles. While work is ongoing to understand the LPI coupling between ranks speckles, one approach to predicting the onset of LPI is the independent hot spot model which describes the speckles statistically.[7] Using the independent hot spot model, the critical beam intensity can be calculated at which the onset of laser plasma instabilities such as SRS and SRS become large. Since the critical onset depends on plasma wave damping, the onset for SRS should vary with $k\lambda_D$, although other experiments and theory suggest that damping could be reduced by electron trapping.[8] Experiments at the Omega laser have been conducted to determine the critical onset for SRS in hohlraum plasmas. Figure 2c shows a plot of laser intensity versus the plasma gas-fill density normalized to the critical density n_e/n_c . The data maps out two regions, that in which the SRS reflectivity is greater than 10% represented by the solid circles, and that in which SRS reflectivity is below 1%, the open circles. The data show a clear delineation between the two regions where a dashed line is drawn to guide the eye. The data show a jump in the SRS reflectivity dependent on laser intensity and plasma density. The density axis represents $k\lambda_D$ where a decrease in density is an increase in $k\lambda_D$. However, electron temperature must be used to get the exact values of $k\lambda_D$. Work is underway to calculate those temperatures via radiation hydrodynamic simulations. In either case, the data show that a sharp onset in SRS reflectivity as either intensity is raised or $k\lambda_D$ is increased.

5. Conclusions

Two strategies for reducing SRS in hohlraum plasma have successfully been demonstrated. The addition of a high Z dopant to a gas filled hohlraum does decrease the backscattered laser energy in the gas fill. This has also been observed in measurements of the soft xray spectrum from gas filled hohlraums. While it may not be possible to use a high-Z gas as a dopant in NIF ignition cryogenic targets, a high-Z dopant might be incorporated in target designs with a low-Z solid or foam liner. A high-Z gas dopant may be used to mitigate SRS in non-cryogenic targets. It has also been shown that increasing $k\lambda_D$ in the gas fill allows higher laser intensities before the onset of SRS. To incorporate either of these mitigation strategies into a NIF ignition target requires substantial radiation-hydrodynamic design work, and is beyond the scope of this paper.

References

- [1] R. M. Stevenson *et al.*, Physics of Plasmas **11**, 2709 (2004).
- [2] E. M. Epperlein, Physical Review Letters **65**, 2145 (1990).
- [3] A. Schmitt, and R. S. B. Ong, Journal of Applied Physics **54**, 3003 (1983).
- [4] A. J. Schmitt, and B. B. Afeyan, Physics of Plasmas **5**, 503 (1998).
- [5] P. M. Lushnikov, and H. A. Rose, Plasma Physics and Controlled Fusion **48**, 1501 (2006).
- [6] P. M. Lushnikov, and H. A. Rose, Physical Review Letters **92**, 255003 (2004).
- [7] H. A. Rose, and D. F. Dubois, Physics of Fluids B (Plasma Physics) **5**, 590 (1993).
- [8] D. S. Montgomery *et al.*, Physics of Plasmas **9**, 2311 (2002).